

Experimental Investigation of Demineralization and Remineralization of Human Teeth Using Infrared Photothermal Radiometry and Modulated Luminescence

Raymond J. Jeon^{a,b}, Adam Hellen^{a,b}, Anna Matvienko^{a,b}, Andreas Mandelis*^{a,b}, Stephen H. Abrams^b,
Bennett T. Amaechi^c

^aCenter for Advanced Diffusion Wave Technologies, Department of Mechanical and Industrial Engineering, University of Toronto, 5 King's College Road, Toronto, Ontario, M5S 3G8, Canada;

^bQuantum Dental Technologies, 748 Briar Hill Avenue, Toronto, Ontario, M6B 1L3, Canada;

^cDepartment of Community Dentistry, University of Texas Health Science Center at San Antonio, 7703 Floyd Curl Drive, San Antonio, Texas 78229-3900, USA

ABSTRACT

Photothermal radiometry (PTR) and modulated luminescence (LUM) were applied to detect and monitor the demineralization of root and enamel surfaces of human teeth to produce caries lesions and the subsequent remineralization of the produced lesions. The experimental set-up consisted of a semiconductor laser (659 nm, 120 mW), a mercury-cadmium-telluride IR detector for PTR, a photodiode for LUM, and two lock-in amplifiers. A lesion was created on a 1-mm X 4-mm rectangular window, spanning root to enamel surface, using an artificial caries lesion gel to demineralize the tooth surface and create small carious lesions. The samples were subsequently immersed in a remineralization solution. Each sample was examined with PTR/LUM on root and enamel before and after treatment at times from 1 to 10 days of demineralization and 2 to 10 days of remineralization. PTR/LUM signals showed gradual and consistent changes with treatment time. At the completion of the experiments, transverse micro-radiography (TMR) analysis was performed to correlate the PTR/LUM signals to depth of the carious lesions and mineral losses. In this study, TMR showed good correlation with PTR/LUM. It was also found that treatment duration did not correlate well to any technique, PTR/LUM, or TMR, which is indicative of significant variations in demineralization - remineralization rates among different teeth.

Keywords: photothermal radiometry, luminescence, demineralization, remineralization

1. INTRODUCTION

Non-invasive evaluation of biological tissues has become a key priority of cutting-edge optical methodologies emerging in the area of biomedical diagnostics during the past decade. Among those techniques, coupled-field (photoacoustic and photothermal) techniques recently attracted much attention since the secondary (acoustic or thermal) signal detection can significantly increase resolution of pure optical diagnostics and allow comprehensive and simultaneous analysis of optical and thermal properties of tissue during laser irradiation.

Frequency-modulated photothermal radiometry (PTR) applied in this study is based on the thermal infrared response of a medium to modulated laser irradiation following optical-to-thermal energy conversion. Following photon migration and scattering, the absorbed fraction of the diffusive light creates an oscillatory temperature (thermal-wave) field, which is detected radiometrically. The generated signals carry subsurface information in the form of a temperature depth integral, allowing analysis of the medium well below the range of optical imaging.

*mandelis@mie.utoronto.ca

In PTR applications to turbid media, such as hard dental tissue, material property and depth information are obtained in two distinct modes: conductively, from near-surface distances (~ 5-500 μm) controlled by the thermal diffusivity of enamel and the modulation frequency of the laser beam intensity; and radiatively, through mid-infrared blackbody emissions from considerably deep regions commensurate with the optical penetration of the diffusely scattered laser optical field, a diffuse photon-density wave (several mm).^{1,2} By optimizing the wavelength and modulation frequency of the PTR signal one is able to examine and probe the entire region of wave propagation, from the near-surface phenomena (higher frequencies) up to at least 5 mm below the enamel surface (lower frequencies).³ At low frequencies (< 10 Hz) the conductive component of heat transfer usually dominates, whereas at high frequencies (> 100 Hz), the radiative component becomes significant. When used with teeth, PTR has the ability to provide depth profilometric information on the status of carious lesions.

Dental caries or tooth decay is a dynamic process with periods of demineralization after exposure to acids and remineralization when exposed to neutral oral fluids. Lesions form and grow with repeated exposure to acidic solutions and inadequate time for remineralization. Detection and monitoring of early carious lesions has become an essential part of dental diagnostic research aimed to transform the current restorative approach to preventive dentistry.⁴⁻⁹ In fact, early carious lesions, where the demineralization of the enamel crystal structure has just begun, are not detectable by conventional visual diagnostics or dental radiographs. In an effort to improve detection accuracy and to use non-radiographic methods, novel methods for early detection of carious lesions based on the laser-induced fluorescence (or luminescence) were introduced.^{10,11} However, the fluorescence phenomenon is caused by porphyrins in oral bacteria present in carious tissue and can not provide accurate information on the presence and amount of tooth tissue demineralization.¹² Recent reviews show that these new techniques do not present enough evidence to be recommended as a substitute for traditional techniques, but might provide additional quantitative information for the evaluation of caries activity and risk assessment.¹⁰

Pulsed laser infrared photothermal radiometry was applied to dental enamel evaluation.^{13,14} However, the temporal decay of the thermal pulse represents only one signal channel available for analysis, requiring additional independent measurements when a set of parameters is evaluated. Moreover, pulsed heating mode leads to a considerable amount of laser energy deposition, thus increasing temperature of the irradiated tissue significantly and preventing in-vivo implementation of tissue diagnostics.

The depth-profilometric frequency-domain photothermal radiometry was recently applied toward the inspection of dental defects.^{15,16} Later, the technique was coupled with modulated luminescence (LUM) as a dual-probe method.^{1,3,16,17} The introduction of modulated luminescence simultaneously with PTR,^{2,16} revealed the existence of two relaxation lifetimes originating in the hydroxyapatite of dental enamel. Variations in LUM emission fluxes and lifetimes between healthy and carious enamel were shown to have a limited depth profilometric character.^{1,3} A combination of PTR and LUM has been developed into an analytical caries detection tool of combined specificity and sensitivity substantially better than the fluorescent, radiographic and visual methodologies.³ Furthermore, PTR has been shown to have the potential to detect early interproximal lesions, which cannot be detected by conventional dental X-rays.¹⁷ Our previous studies have also shown that temperature rise in the tissues following modulated laser heating is usually less than 1°C in magnitude which will not harm vital pulp tissue. This makes PTR a very promising tool for non-invasive in-vivo detection and monitoring of early tissue abnormalities, including dental demineralization.

The purpose of this study was to assess the ability of PTR and LUM to detect and monitor the degree of demineralization and remineralization of early-stage carious lesions on root and enamel of human teeth. Lesions were artificially created by demineralization-remineralization agents with various treatment times and were scanned by PTR/LUM. These experimental results were compared with mineral loss and lesion depth determined by the current 'gold standard' for measurement of mineral changes in tooth tissue, transverse micro-radiography (TMR), and correlation coefficients were calculated between the methods.

2. EXPERIMENTAL METHODOLOGY

2.1 Sample preparation

Human teeth with healthy surfaces and no visible defects were used in the experiments. Each of fourteen samples was cleaned and mounted on LEGO blocks. This allowed the teeth to be separated and remounted into the exact position during repeated measurements. Between the experiments, the samples were stored in a humid container.

Each sample was painted with two coats of acid-resistant polish except for a rectangular window (1 mm (W) × 4 mm (H)) extending from enamel to root as shown in Fig. 1. Demineralization or remineralization of each sample was carried out in 25 ml of treatment solution in a 50-ml polypropylene test tube, with the sample immersed upside down such that only the exposed rectangular window would be immersed in solution. Demineralization to create an artificial caries lesion was achieved using an acidified gel system,¹⁸ consisting of 0.1 M lactic acid solution gelled to a thick consistency with 6 %w/v hydroxyethylcellulose (Aldrich, Dorset, UK) and the pH adjusted to 4.5 with 0.1 M NaOH. The remineralization solution¹⁹ used in this study consisted of MgCl₂•6H₂O (0.03 g/L), K₂HPO₄ (0.121 g/L), KH₂PO₄ (0.049 g/L), KCl (0.625 g/L), calcium lactate (3.85 g/L), fluoride (0.05 ppm), methyl-*p*-hydroxybenzoate (2.0 g/L), and sodium carboxymethylcellulose (0.4 g/L). The pH was adjusted to 6.7 using KOH. Each sample was treated with different demineralization and remineralization time period. Six samples were demineralized for up to 10 days for enamel and 5 days for root, and then remineralized for 2, 5 and 10 days (2 samples per each time period). The remaining 8 samples were only demineralized for either 1, 2, 5 (both enamel and root) or 10 days (enamel only). Details of the sample treatment matrix are given in our study.²⁰

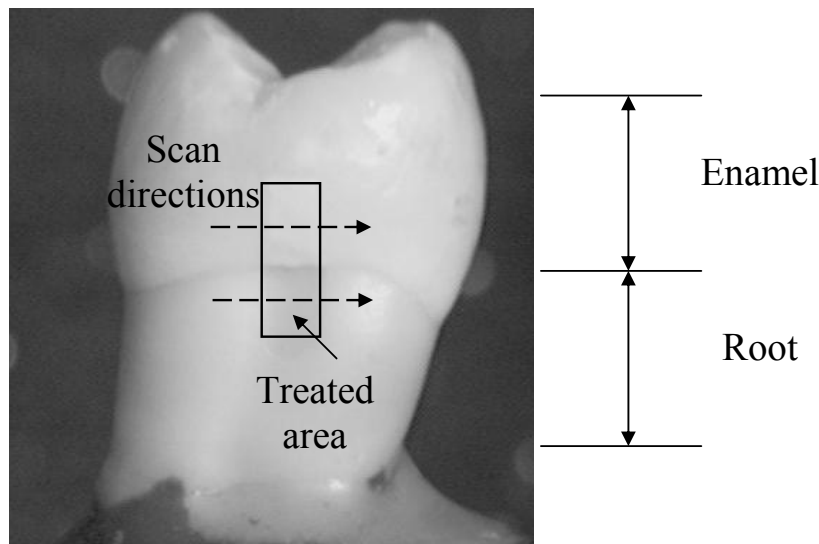


Fig. 1. Tooth sample. The area in the middle is a treated spot. The upper part of the segment is enamel, the lower is the root. Arrows show line-scan directions. The area outside the treated spot was covered with nail polish during treatments.

A sample tooth was taken out of the container before an experiment and was exposed to air for about 20 minutes for drying, in order to avoid causing signal drift due to small humidity changes on the enamel surface. Then, the tooth on the LEGO base was placed on the micro-positioning stage, the laser was turned on and another 10 minutes lapsed before measurements commenced, so that the sample surface might be stabilized thermally. As reported earlier,^{1,17} after 20 minutes the effect of hydration on optical properties, such as light scattering and fluorescence, as well as on thermal properties, is minimal or negligible for measurements lasting less than two hours.

2.2 PTR/LUM experimental setup

The experimental set-up is shown in Fig. 2. A semiconductor laser diode emitting at 659 nm (Mitsubishi ML101J27, maximum power: 120 mW) with the laser beam 150 μm was used in as a signal source. A diode laser driver (Thorlab, LDC 210) triggered by the built-in function generator of the lock-in amplifier (EG&G 7265) modulated the laser current harmonically. The modulated infrared PTR signal from the tooth was collected and focused by two off-axis paraboloidal mirrors (Melles Griot 02POA017, Rhodium coated) onto a Mercury Cadmium Telluride (HgCdTe or MCT) detector (Judson Technologies J15D12, spectral range: 2 to 12 μm , peak detectivity $D^* \approx 5 \times 10^{10} \text{ cm Hz}^{1/2} \text{ W}^{-1}$ at ca. 12 μm). Before being sent to the lock-in amplifier, the PTR signal was amplified by a preamplifier (Judson Technologies PA-300). For the simultaneous measurement of PTR and LUM signals, a lens (focal length: 100 mm) was placed above the off-axis paraboloidal mirrors where it did not block infrared energy passage between the mirrors. The collected modulated luminescence was focused onto a silicon photodiode. A cut-on colored glass filter (Oriel 51345, cut-on wavelength: 715 nm) was placed in front of the luminescence photodetector to block laser light reflected or scattered by the tooth. For monitoring the modulated luminescence, another lock-in amplifier (Stanford Research System, SR830) was used. Both lock-in amplifiers were controlled by a computer via RS-232 ports.

Two kinds of experiments were performed on both enamel and root of each sample: line scans in which the laser was scanned across the treated area of a tooth, in the direction of the white arrows shown in Fig. 1 under normal incidence at fixed frequencies; and a frequency scan, which measured the PTR and LUM signals at the center of each treated area. The detailed description of the frequency scans can be found in our study.²⁰ There was a 15-s time delay between measurements between spatial coordinate scans to allow for thermalization of the tooth surface, that time interval being necessary for thermally stabilizing the signals. Following completion of PTR and LUM measurements, all samples were subjected to TMR analysis to determine the caries lesion parameters of mineral loss and lesion depth as described below.

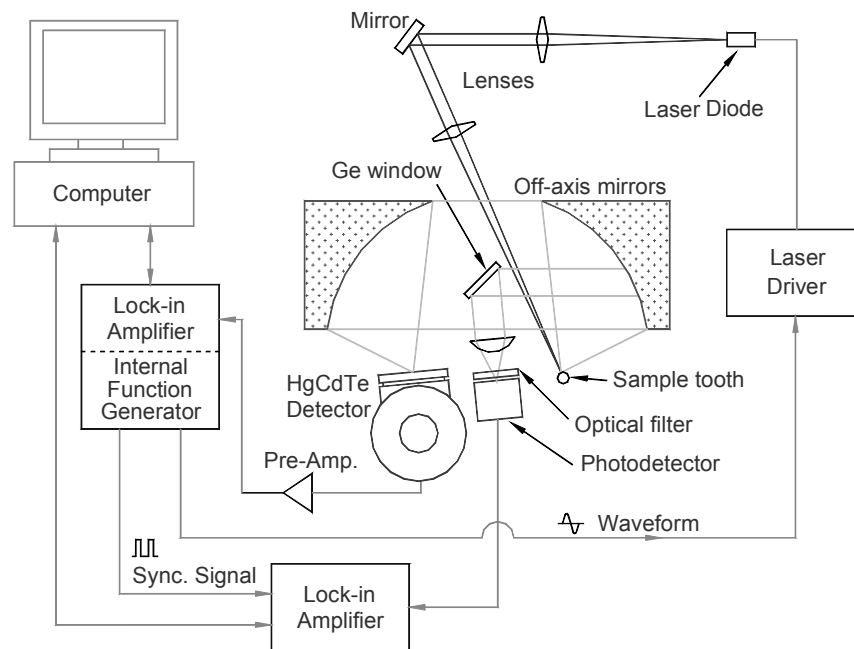


Fig. 2. PTR/LUM experimental setup.

2.3 Transverse Microradiography (TMR) and image analysis

Following PTR/LUM scanning, the teeth samples were carefully sectioned, using hard tissue cutting machine (Microtome, Scientific Fabrication, Lafayette, USA), to produce an enamel (or root) slab approximately 100 μm thick. These sections were placed in a specially fabricated radiographic plate-holding cassette, incorporating an aluminium step

wedge (10 steps of 24.5 μm thickness). The cassette was loaded with type 1A high resolution glass X-ray plates (IMTECH Ca. USA) and placed into a Phillips x-ray generator system set up for this purpose. This apparatus is equipped with a copper target and nickel filter, producing monochromatic radiation of wavelength appropriate for hydroxyapatite (184 Angstroms). The plates were exposed for 10 minutes at an anode voltage of 20kV and a tube current of 10 mA, and then processed. Processing consisted of a 5 minute development in Kodak HR developer and 15 min fixation in Kodak Rapid-fixer before a final 30 minute wash period. After drying, the microradiographs were subjected to visualization and image analysis using a computer program, TMRW (Version 2.0.27.2, Inspektor Research Inc., Amsterdam, Netherland). The hardware was a Leica DMR optical microscope linked via a Sony model XC-75CE CCTV camera to a 90 MHz Dell™ Pentium Personal Computer. The enhanced image of the microradiograph was analyzed under standard conditions of light intensity and magnification and processed, along with data from the image of the step wedge, by the TMRW program. By this method, the parameters of integrated mineral loss (Δz , vol%. μm) and lesion depth (LD, μm) were quantified.

3. RESULTS AND DISCUSSION

During the series of treatments, artificial carious lesions were created on root and enamel surfaces of human teeth with demineralization gel and were partially reversed with subsequent remineralization treatment. The full cycle was examined by photothermal radiometry (PTR) and modulated luminescence (LUM). PTR amplitude and phase line-scans exhibited gradual and consistent changes with treatment time. The example of the experimental PTR line-scan results are presented in Figs. 3 and 4. The tooth sample was demineralized sequentially up to 10 days followed by remineralization for 10 days. The data sets are shown before treatment, after 1, 2, 5 and 10 days of demineralization, and after 2, 5 and 10 days of remineralization. The rest of the treated samples exhibited similar behavior. The PTR amplitude showed gradual increase with increasing demineralization time in the $\sim 2\text{-mm}$ region which had been exposed to the demineralization gel, and reversed direction (decreased slightly) after remineralization. This is typical of PTR amplitude as it is related to the increase in microporosity of the surface layer, leading to the visual appearance of white spot lesions. An increase in porosity leads to increased scattering in the lesion layer, thus producing higher signal magnitude due to energy confinement in the demineralized layer. With layer growing in thickness during demineralization, the integrated amount of energy increases, which results in gradual increase of PTR amplitude with treatment time. Once remineralization begins, the signal amplitude begins to decrease slowly. The relatively slow response to the remineralization solution may occur because it is difficult to significantly remineralize dental tissue at relatively short remineralization times.

PTR phase also exhibited gradual changes after each treatment. In general, the PTR phase lag (Figs. 3 and 4) decreased throughout demineralization and then reversed direction (started increasing) for remineralization cycle. The phase curves are a very sensitive signal channel showing evidence of a growing demineralization lesion: a larger phase lag in the untreated tooth is due to the relatively low incident photon scattering which allows a longer optical attenuation depth and larger phase lag of the generated photothermal response.²

An important difference between the kinetics of the enamel and root PTR changes is the rate of the PTR response difference at the end of demineralization treatment. The enamel amplitude shifts significantly between 5 and 10 days of treatment, while the root amplitude shows no change during this period. The PTR phase lag for enamel kept on decreasing with longer demineralization times and increased after the onset of the 10-day remineralization cycle, while the root phase lag already began to increase at the last demineralization measurement. One of the possible explanations of this phenomenon corresponds to the known fact that the root tissue is less mineralized compared to enamel and therefore more susceptible to acid dissolution than enamel. Thus, the fast dissolution of the root results in early saturation of the demineralization gel with the inorganic ions dissolved from the lesion. Saturation of the gel adjacent to the lesion surface causes a change in concentration gradient of inorganic ions, resulting in inward diffusion of the ions back into the lesion causing net remineralization of the surface layer instead of demineralization. As the remineralization process begins, the direction of PTR signal changes for enamel. This occurs because remineralization stops the dissolution of the mineral and the signal shifts towards healthy levels. On the other hand, the PTR signal of the root continues to move toward the healthy levels due to the increase in mineral content. This hypothesis is also supported by the TMR cross-sectional images in Fig. 5 and 6. The surface layer can already be seen in the root image of the sample treated with demineralization solution only for 5 days (Fig. 5). The sample remineralized for 10 days shows a well-defined mineralized surface layers for both enamel and root (Fig. 6).

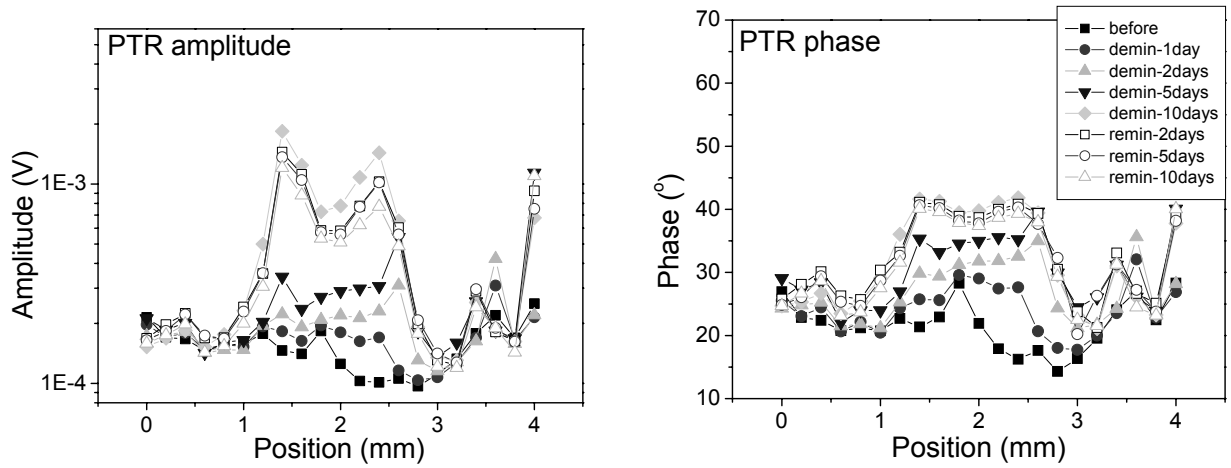


Fig.3. Enamel PTR line scans at modulation frequency 10 Hz: amplitude and phase lag.

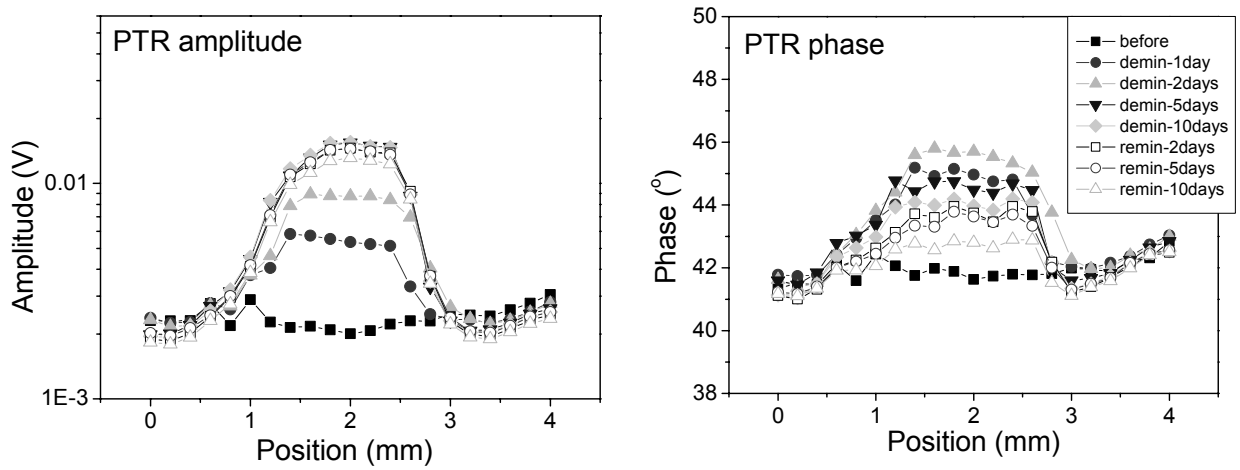


Fig.4. Root PTR line scans at modulation frequency 10 Hz: amplitude and phase lag.

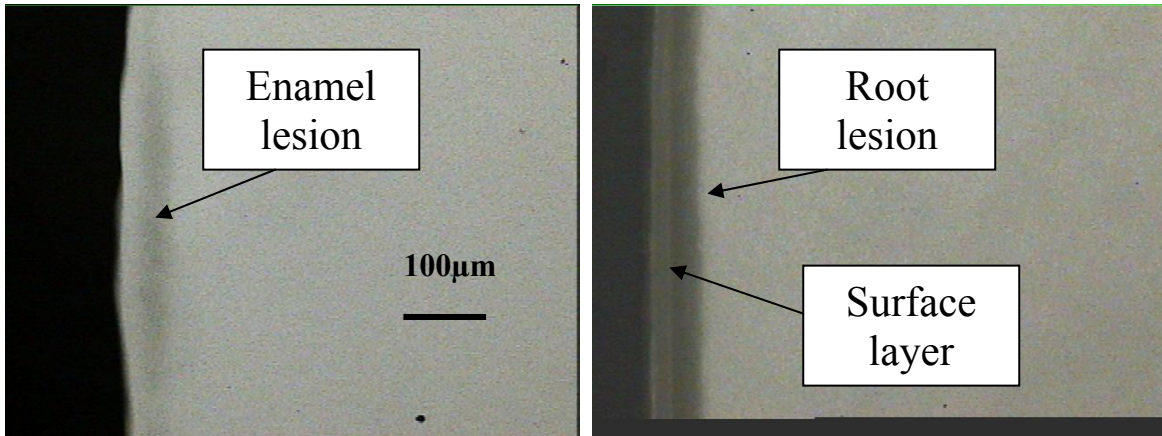


Fig.5. TMR images of sample demineralized for 5 days.

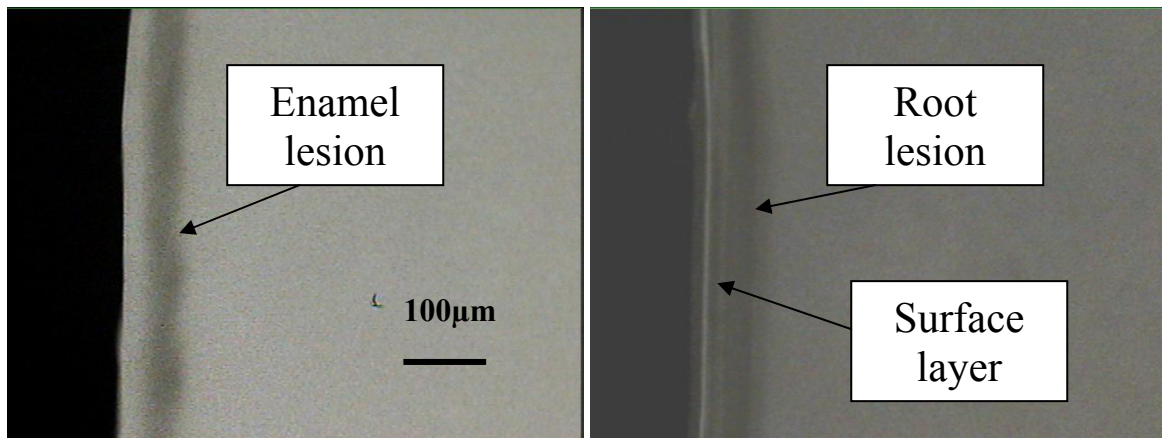


Fig.6. TMR images of sample demineralized for 10 days and remineralized for 10 days.

The LUM amplitude and phase show less contrast than their PTR counterparts, a fact consistent with previously reported studies on LUM.^{2,17} Comparing the LUM signals from root and enamel (Figs. 7 and 8), the LUM amplitude at ~ 2 mm region of enamel exposed to the demineralization gel clearly decreased with respect to the unexposed baseline after 10 days of demineralization while almost no change was observed in the root. After 10-day remineralization, the LUM amplitude increased for both root and enamel as shown in Figs. 7 and 8. The increase of the LUM amplitude on root was much larger than that on enamel, which is also consistent with trends in the PTR signal amplitude changes. A signal reversal amplification factor in LUM may be a combination of enamel recrystallization and decreased water diffusion in the hydroxyapatite microstructure during the remineralization process, yielding higher sensitivity of the LUM amplitude to remineralization than that expected from each individual process acting independently.

The detailed analysis of demineralization-remineralization kinetics based on the PTR/LUM frequency scans can be found in our recent study.²⁰

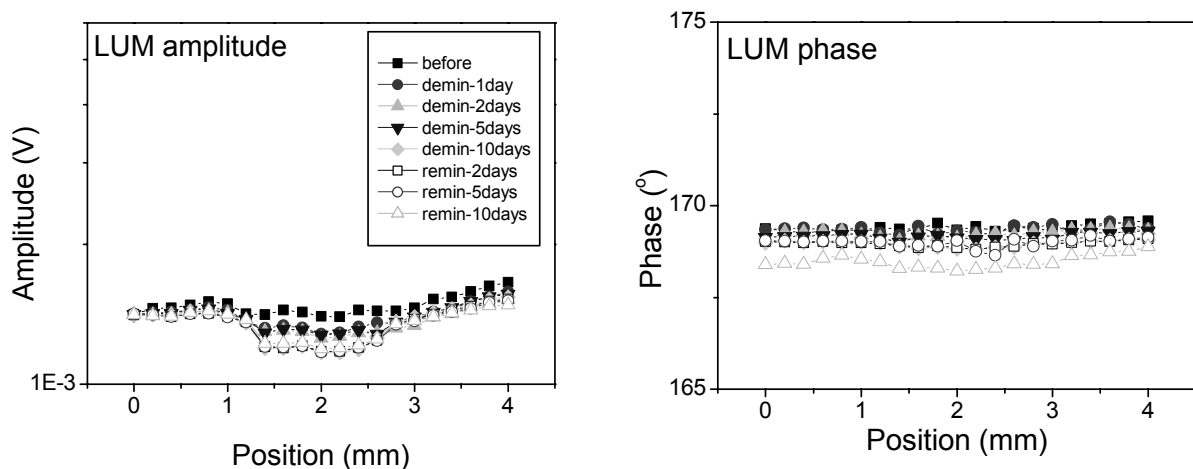


Fig.7. Enamel LUM line scans at modulation frequency 10 Hz: amplitude and phase lag.

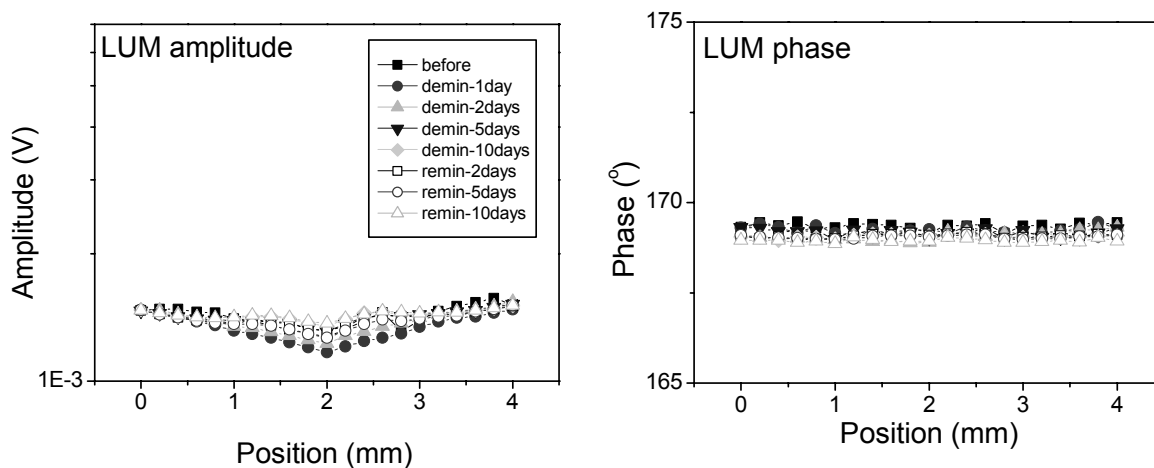


Fig.8. Root LUM line scans at modulation frequency 10 Hz: amplitude and phase lag.

The investigated tooth samples underwent subsequent TMR analysis. The mineral loss was computed as the difference in volume percent of mineral between sound and demineralized tissue integrated over the lesion depth. The lesion depth was assessed as the distance from the measured sound tissue surface to the location in the lesion at which the mineral content is larger than 95% of the mineral content in sound tissue. These were statistically compared and correlated to the PTR and LUM signal.

The correlation coefficient was calculated on the basis of the results for the set of the teeth as follows:

$$\rho(x, y) = \frac{\text{cov}(x, y)}{\sigma_x \sigma_y}, \quad -1 \leq \rho \leq 1 \quad (1)$$

$$\text{cov}(x, y) = \frac{1}{n} \sum_{j=1}^n (x_j - \mu_x)(y_j - \mu_y) \quad (2)$$

where μ is the mean value and σ is the standard deviation of the populations x and y . The results of the correlation are presented in Table 1 and Table 2. It is evident that TMR gives good correlation with both enamel and root PTR signal (Table 1). The same trend was found for the LUM signal correlation, especially for enamel lesions.

Table 1. Correlation coefficients between the PTR amplitude and phase and the mineral loss and the lesion depths by the TMR measurements.

<i>Correlation coefficient</i>			PTR amplitude @10Hz			
			Enamel		Root	
			last demin	last remin	last demin	last remin
TMR	Enamel	Mineral loss	0.64	0.65		
		Lesion depth	0.60	0.59		
	Root	Mineral loss			0.71	0.68
		Lesion depth			0.53	0.47

<i>Correlation coefficient</i>			PTR phase @10Hz			
			Enamel		Root	
			last demin	last remin	last demin	last remin
TMR	Enamel	Mineral loss	0.46	0.45		
		Lesion depth	0.54	0.51		
	Root	Mineral loss			0.26	0.21
		Lesion depth			0.38	0.27

Table 2. Correlation coefficients between the LUM amplitude and phase and the mineral loss and the lesion depths by the TMR measurements.

<i>Correlation coefficient</i>			LUM amplitude @10Hz			
			Enamel		Root	
			last demin	last remin	last demin	last remin
TMR	Enamel	Mineral loss	-0.65	-0.70		
		Lesion depth	-0.83	-0.86		
	Root	Mineral loss			-0.17	-0.08
		Lesion depth			0.21	0.31

<i>Correlation coefficient</i>			LUM phase @10Hz			
			Enamel		Root	
			last demin	last remin	last demin	last remin
TMR	Enamel	Mineral loss	-0.55	-0.46		
		Lesion depth	-0.50	-0.46		
	Root	Mineral loss			0.31	0.013
		Lesion depth			0.23	-0.04

Overall, in view of the good correlation of PTR/LUM with the mineral loss or the lesion depth measured with TMR results, it can be concluded that PTR/LUM is capable of monitoring artificially created carious lesions, their evolution during demineralization, as well as their reversal upon remineralization. It was also found that cumulative treatment time did not correlate well with either PTR/LUM or TMR which is indicative of significant variations in demineralization-remineralization rates among different teeth as well as across each individual tooth.

REFERENCES

- ¹ R. J. Jeon, A. Mandelis, V. Sanchez, and S. H. Abrams, "Non-intrusive, Non-contacting Frequency-Domain Photothermal Radiometry and Luminescence Depth Profilometry of Carious and Artificial Sub-surface Lesions in Human Teeth," *J. Biomed Opt.* **9**, 804-819 (2004).
- ² L. Nicolaidis, C. Feng, A. Mandelis, and S. H. Abrams, "Quantitative dental measurements by use of simultaneous frequency-domain laser infrared photothermal radiometry and luminescence," *Appl. Opt.* **41**, 768-777 (2002).
- ³ R. J. Jeon, C. Han, A. Mandelis, V. Sanchez, and S. H. Abrams, "Diagnosis of Pit and Fissure Caries Using Frequency-Domain Infrared Photothermal Radiometry and Modulated Laser Luminescence," *Caries Res.* **38**, 497-513 (2004).
- ⁴ G. N. Jenkins, "Recent changes in dental caries," *Br. Med. J.* **291**, 1297-1298 (1985).
- ⁵ D. Ricketts, E. Kidd, K. Weerheijm, and H. de Soet, "Hidden caries: What is it? Does it exist? Does it matter?," *Int. Dent. J.* **47**, 259-265 (1997).
- ⁶ D. McComb and L. E. Tam, "Diagnosis of Occlusal Caries: Part I. Conventional Methods," *J. Can. Dent. Assoc.* **67**, 454-457 (2001).
- ⁷ K. J. Anusavice, "Need for Early Detection of Caries Lesions," *A United States Perspective in Early Detection of Dental Caries II Proc. 4th Annual Indiana Conf.* G. Stookey ed., pp. 13-30 (2001).
- ⁸ A. F. Zandoná, "Diagnostic tools for early caries detection," *JADA* **137**, 1675-1684 (2006).
- ⁹ S. Tranæus, X.-Q. Shi and B. Angmar- Månsson, "Caries risk assessment: methods available to clinicians for caries detection." *Community Dent Oral Epidemiol* **33**, 265-273 (2005).
- ¹⁰ R. Hibst, and K. Konig, "Device for Detecting Dental Caries," US Pat., 5,306,144 (1994).
- ¹¹ R. Hibst, R. Gall and M. Klafke, "Device for the Recognition of Caries, Plaque or Bacterial Infection on Teeth," US Pat., 6,024,562 (2000).
- ¹² H. M. Alwas-Danowska, A. J. M. Plasschaert, S. Suliborski, and E. H. Verdonshot, "Reliability and validity issues of laser fluorescence measurements in occlusal caries diagnosis," *J. Dentistry* **30**, 129 – 134 (2002).
- ¹³ D. Fried, W. Seka, R.E. Glana, J.D.B. Featherstone, *Opt. Eng.* **35**, 1976-1984 (1996).
- ¹⁴ M.J. Zuerlin, D. Fried, J.D.B. Featherstone, W. Seka, *IEEE J. Quantum Electron.* **5**, 1083-1089 (1999).
- ¹⁵ A. Mandelis, L.Nicolaidis, C. Feng, and S. H. Abrams, "Novel Dental Depth Profilometric Imaging Using Simultaneous Frequency-Domain Infrared Photothermal Radiometry and Laser Luminescence," *Proc. SPIE* **3916**, 130-137 (2000).
- ¹⁶ L. Nicolaidis, A. Mandelis, and S. H. Abrams, "Novel Dental Dynamic Depth Profilometric Imaging Using Simultaneous Frequency-Domain Infrared Photothermal Radiometry and Laser Luminescence," *J. Biomed. Opt.* **5**, 31-39 (2000).
- ¹⁷ R. J. Jeon, A. Matvienko, A. Mandelis, S. H. Abrams, B. T. Amaechi, and G Kulkarni, "Detection of Interproximal Demineralized Lesions on Human Teeth *in vitro* Using Frequency-Domain Infrared Photothermal Radiometry and Modulated Luminescence," *J. Biomed Opt.* **12**, 034028 (2007).
- ¹⁸ B. T. Amaechi, S. M. Higham, and W. M. Edgar, "Factors affecting the development of carious lesions in bovine teeth *in vitro*," *Archs. Oral Biol.* **43**, 619-628 (1998).
- ¹⁹ B. T. Amaechi and S. M. Higham, "Quantitative light-induced fluorescence: A potential tool for general dental assessment," *J. Biomed. Opt.* **7**, 7-13 (2002).
- ²⁰ R. J. Jeon, A. Hellen, A. Matvienko, A. Mandelis, S. H. Abrams, and B. T. Amaechi, "In vitro Detection and Quantification of Enamel and Root Caries Using Infrared Photothermal Radiometry and Modulated Luminescence," *J. Biomed Opt.*, under review.